23rd ABCM International Congress of Mechanical Engineering
December 6-11, 2015, Rio de Janeiro, RJ, Brazil

STRESS ANALYSIS OF A FAILED STAINLESS STEEL FEMORAL PLATE

João Paulo Pascon
Carlos Antonio R. P. Baptista
José Benedito Marcomini
EEL/USP – Escola de Engenharia de Lorena, University of São Paulo, Estrada Municipal do Campinho, Lorena/SP, Brazil
jppascon@usp.br, carlos.baptista@usp.br, jmarcomini@usp.br

Abstract. *Surgical implants are exposed to severe working conditions and therefore a wide range of failure mechanisms may occur, including fatigue, corrosion, wear, fretting and combinations of them. An 83-year-old patient suffered an oblique femoral shaft fracture due to a fall at home. The plate fractured along one of the combination holes, approximately aligned to the femur fracture and with no screw locked into it. A FEM model of the orthopaedic implant was developed in order to estimate the stress distribution along the femoral plate. The numerical simulation was done with a computer code developed by one of the authors. The adopted finite element is the isoparametric solid tetrahedron of quadratic order. Two models have been numerically analyzed: one with four screws, and one with three screws (that is, with an empty hole on the femoral plate). The distribution of the von Mises stress was obtained at the end of the simulation. The numerical results show that the removal of one of the screws leads to a stress increase around the empty hole. The maximum value of the von Mises stress for the model with an empty hole is 125.3 MPa and occurs around the hole. For the model with four screws, the von Mises stress at the same point is 39.8 MPa. Thus, the stress concentration factor, considering the present model, is 3.15.*

Keywords: *Femoral Plate, Stress Analysis, Failure Analysis, Fatigue, Stainless Steel*

1. INTRODUCTION

The femur is the longest and strongest bone in the human body. The femoral shaft is the lengthy part of the femur, and a break along it is called femoral shaft fracture (Bucholz and Jones, 1991). The annual incidence of midshaft femur fractures was estimated to be approximately 10 per 100,000 person/year. The main causes are high-energy collision due to motor vehicle crash and, in older adults (mainly those over age 75 years), low energy falls. These typically occur in the home and account for 65% of the fractures (Weiss *et al.*, 2009; Hedlund and Lindgren, 1986). Femur fractures vary greatly, depending on the kind and intensity of the loading that causes the break. One of the most common type of femoral shaft break is the oblique fracture, were the fracture plane is inclined in relation to the bone axis line. Most femoral shaft fractures require surgery to heal. The external fixation is a temporary treatment often adopted when the skin and muscles have been injured. Orthopaedic devices such as the intermedullary nailor a compression plate are used in surgical procedures for internal fixation of fractures (Sudhakar, 2005). The latter is classified as dynamic compression plate (DCP) or locking compression plate (LCP). In both cases, the bone fragments are reduced into their normal alignment and held together with screws and the plate is attached to the outer surface of the bone. Another approach, described as the "biological internal fixation", employs flexible fixators and tolerates some mobility of the interface of fracture (Perren, 2002).

The main difference between the compression plates is that in DCP the screws must be tightened into the holes, resulting in high compressive forces between bone and plate that may cause vascular damage to the undersurface bone tissue. The more recent LCP introduced the combination hole, which allows the load to be transmitted through screw-plate system without compression between plate and bone surface when the conical thread holes are used (Kanchanomai *et al.*, 2008; Stevens and Duis, 2008). Surgical implants are exposed to severe working conditions, including mechanical loading (cyclic and shock), chemical aggression (body fluids) and the static or dynamic contact between the implant materials or the state of implant-to-bone contact (Azevedo & Hippert Jr, 2002; Roffey, 2012). The mechanical failures of metallic implants may be influenced by several other factors, including the design, material selection, manufacturing, improper installation, postoperative complications and misuse (Azevedo & Hippert Jr, 2002).

In the present work, a failed femoral plate is considered. An 83-year-old patient suffered an oblique femoral shaft fracture due to a fall at home. A locking compression plate (LCP) employed in the fracture reduction failed after four months and was sent back to the producer. A second LCP of the same type was implanted and also failed after six months. Both implants were manufactured by the same supplier. A failure analysis of the second femoral LCP was performed in a previous paper (Marcomini *et al.*, 2014). A FEM model of the orthopaedic implant was developed in order to estimate the stress distribution along the femoral plate and is presented in this paper. There was no presence of rusts or corrosion on the failed plate surface, which presented a typical stainless steel brightness. The plate fractured along one of the combination holes, see Fig. 1, approximately aligned to the femur fracture and with no screw locked into it. The fractured surfaces were analyzed in order to investigate the macro and microscopic fracture features. Two fracture origins could be found. Probably, both crack fronts nucleated almost at the same time in stress concentration sites. Beach marks observed close to the fracture origins revealed that the fracture mechanism was fatigue.

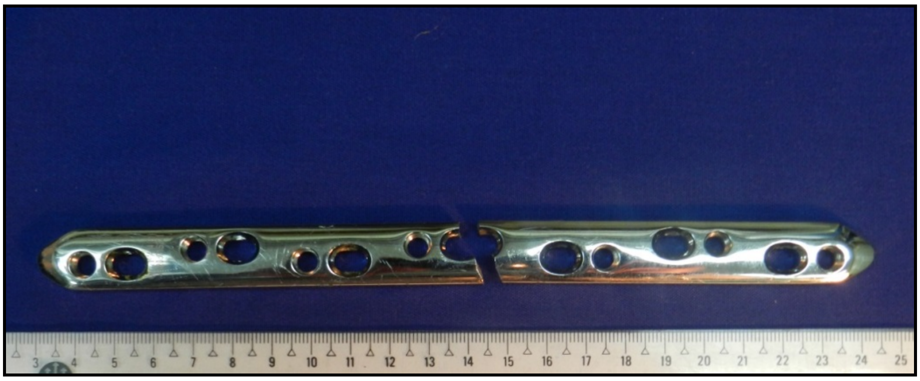

Figure 1. The fractured femoral plate

2. MATERIAL CHARACTERIZATION

The femoral plate steel wet chemical analysis was performed based on ASTM E 353.The results in weight percent are the following: 0.03 C; 17.65 Cr; 15.00 Ni and 0.046 P. The chemical analysis revealed that the LCP femoral plate was manufactured with a stainless steel. Some stainless steel types are commonly used for orthopaedic devices such as AISI 316L, ASTM F 138 and 139 (special type of 316L for medical applications), and ISO 5832-9. Considering the evolution of steels for medical applications the most advanced stainless steel nowadays is the ISO 5832-9, which can be the substitute of ASTM F 138 (Giordani *et al.*, 2004). The chemical composition of the steel used in the femoral plate of this work matches with the ISO 5832-9 except by the higher phosphorus content. The ISO 5832-9 standard chemical composition presents a maximum P content of 0.025%. The sample taken from the fractured femoral plate presented a P content of 0.046%. The LCP steel is not in accordance to ASTM F 138 nor to ASTM F 139. Moreover, this steel does not conform to any standard for316L stainless steel type (ASTM A 240, ASME SA 240, ASTM A 276) because of the higher content of Ni and P. The embrittlement of austenitic steels caused by phosphorus is well known (Castro and Gueussier, 1960), and that is why the phosphorus content in standards, especially for biomedical materials, is limited.

An optical microscope metallographic analysis was performed in order to investigate the microstructure, grain size and sensitization degree. Samples were taken from a parallel position of the femoral plate longitudinal axes. The metallographic analysis revealed that the austenitic grain size of the steel is between 6 and 7 according to ASTM E 112. The microstructure shown in Figure 2 reveals many slip lines and annealing twins, which shows that the material was subjected to cold work The specimens etched with oxalic acid at 1 A/cm^2 for 1.5 min revealed a sensitization pattern similar to “End Grain Pitting I” according to ASTM A 262. Figure 3 shows the optical microscope images of stainless steel sensitized microstructure.

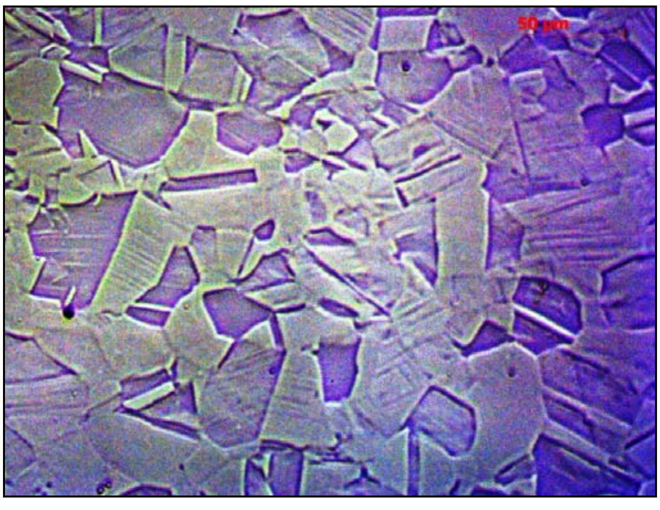

Figure 2. Optical microscope image of the microstructure of the femoral plate stainless steel without etching

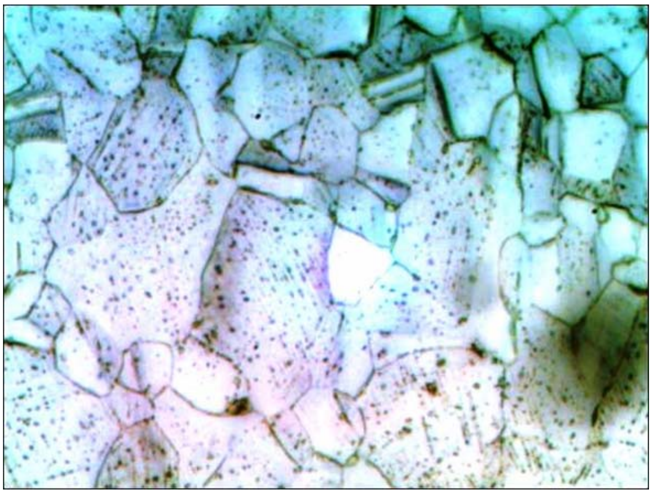

Figure 3. Optical microscope image of the sensitized microstructure of the femoral plate stainless steel after electrolytic etching (oxalic acid at 1 A/cm^2 for 1.5 min) showing carbide precipitation ($Cr_{23}C_6$)-sensitization

Vickers hardness measurements were performed in fifteen points of the femoral plate. The test method was based on ASTM A370 and the applied load was HV0.5. The average hardness value was (288 ± 5) HV. This hardness number is in accordance to the cold deformation suggested by the slip lines present in microstructure. The Vickers hardness number, 288HV, may be converted to tensile strength according to ASTM A 370. This Vickers hardness value corresponds to a tensile strength of the order of 900 MPa. It is known that, after 27% cold deformation, the 316L stainless steel presents yield stress around 900 MPa in tensile test and ultimate tensile strength around 950 MPa (Suyitno *et al.*, 2012). It means that the elongation is low what is typical of a brittle behavior caused by work hardening. A coupon was taken from the LCP and a trapeze shaped cross section specimen was machined and subjected to a quasi-static three point bending load in a universal testing machine. The specimen did not fail by brittle fracture, yet plastically bent instead. The calculated proportional limit stress in bending was approximately 941 MPa. Considering the proportional elastic limit estimated from the bend test and the estimated ultimate strength, 900 MPa, it must be taken into account that there is an associated error in these estimations. Nevertheless, it is possible to deduce that the LCP steel yield strength and ultimate strength present very close values.

3. STRESS ANALYSIS

A stress analysis was done in order to study the influence of the screws on the stress distribution in the femoral plate, as well as the effect of an empty hole on stress distribution. One should remember that the objective here is not to reproduce the femoral plate and the bone with high realism. Due to the geometric complexity, the stress analysis of the femoral plate is performed by means of the finite element method (FEM). The adopted finite element is the isoparametric solid tetrahedron of quadratic order (see Pascon and Coda, 2012 for further details). The numerical simulation has been done with a computer code developed by one of the authors.

The numerical model generated, depicted in Fig. 4, is based on the experimental procedure used in Kanchanomai *et al.* (2008), in which the applied load is oblique and eccentric regarding the femur. In the present simplified model, the bone and the femoral plate are prismatic bars. The bone has a square cross-section, and the femoral plate model has a rectangular cross-section with four holes along the length. As the femoral plate holes are aligned in pairs, two groups of two aligned holes each has been adopted. Regarding the constitutive modeling, the mechanical behavior is governed by the three-dimensional Hooke's law. The applied static force has a magnitude of three times the patient's weight of 60kg (which means 1800 N), which is equivalent to following loading system: normal compressive force of 1767 N, shear force of 343 N, and a bending moment of 97.2 N m (see Fig. 4). To reproduce the boundary conditions of the test presented in Kanchanomai et al. (2008), the base of the bone (y = 0) is clamped, i.e., all the displacements of the points located at the base are restricted. Finally, to simplify the analysis, the interaction among the bone, the screws and the femoral plate is considered rigid.

Two models have been numerically analyzed: one with four screws and one with three screws (that is, with an empty hole on the femoral plate). For the first case, the mesh employed has 18785 nodes and 12096 tetrahedral elements. The mesh of the second model has 18077 nodes and 11520 tetrahedra. The distribution of the von Mises stress is obtained at the end of the simulation. The numerical results show that the removal of one of the screws leads to a stress increase around the empty hole, see Fig. 5. The maximum value of the von Mises stress for the model with an empty hole is 125.3 MPa and occurs around the hole. For the model with four screws, the von Mises stress at the same point is 39.8 MPa. Thus, the stress concentration factor, considering the present model, is 3.15. It should be verified if this stress level is acceptable from the point of view of fatigue. The fatigue endurance limit of austenitic steels under bending could be estimated as 0.37 $S_u \approx$ 361 MPa for the steel used in the femoral plate (Lee *et al.*, 2005). Upon the stress raiser, whereas the austenitic stainless steels in the annealed condition is not notch sensitive, it was observed in the fatigue curves of a cold-drawn 304 stainless steel that the cold-worked condition has much lower fatigue strength if samples are notched, with the fatigue strength decreasing from 760 to about 170 MPa (Brooks, 1992). On the other hand, even if the steel used in the femoral plate is fully-notch sensitive (q = 1), the fatigue stress concentration factor would be not enough to induce crack initiation under usual loading. However, it must be stated that, because of notch sensitivity, the use of cold-worked material may not provide an advantage over annealed material with regard to fatigue strength (Brooks, 1992).

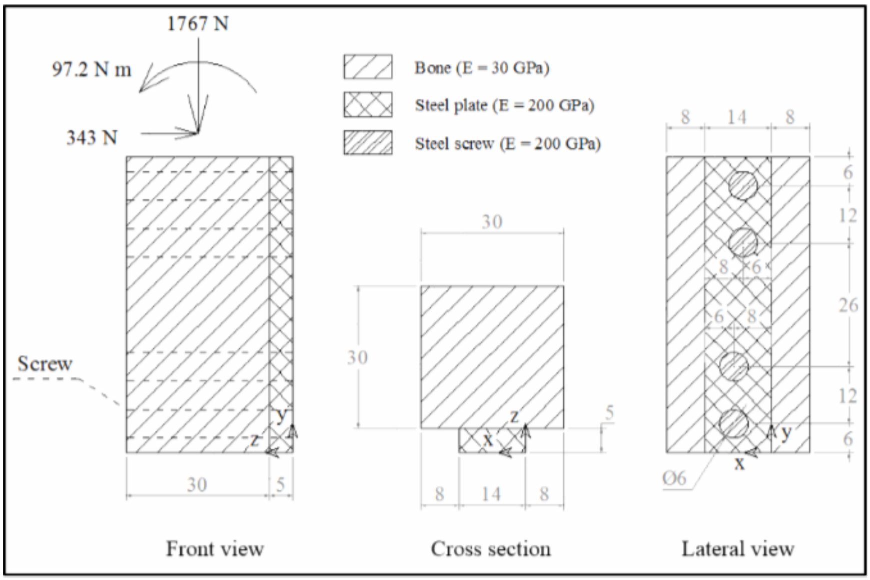

Figure 4. Numerical model generated for the stress analysis of the femoral plate (dimensions in millimeters)

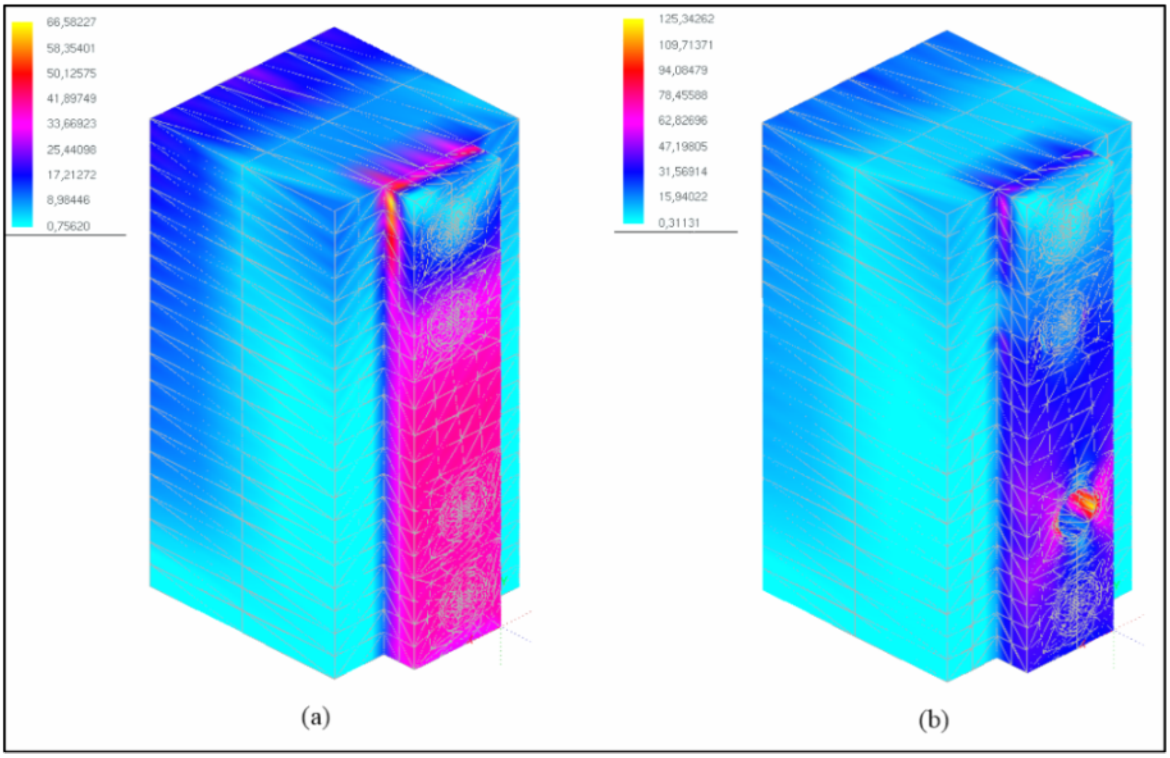

Figure 5. Final von Mises stresses: (a) four screws; (b) three screws with an empty hole

From the stress analysis, it can be inferred that the femoral LCP presents no design problem and the absence of one screw at the analyzed hole is not a critical stress concentration point. The surface finish of the device suggests the complete absence of corrosion influence on the fracture process.

4. CONCLUSION

It is clear from the analysis results that the main mechanisms leading to the fracture of the device were due to non-conformity of the material. The femoral LCP presents no design problem and the absence of one screw at the analyzed hole is not a critical stress concentration point. The stress concentration factor, considering the present model, is 3.15, and even if the material is fully notch sensitive, it is not critical for fatigue. This information should be taken into account during the design process of a similar femoral plate. Although subcritical fatigue crack growth was observed, the poor material quality was decisive to failure. The austenitic stainless steel embrittlement by phosphorus is a well-known phenomenon. Phosphorous content 0.26% over the ASTM F 138/139 superior limit caused segregation in grain boundaries allowing for intergranular brittle crack initiation in stress concentration locus. The cyclic loading (due to walking), inherent to this device, induced the fatigue crack propagation of initiated cracks. The segregation of phosphorus in grain boundaries causes the embrittlement of the steel and may lead to a brittle fracture.

5. ACKNOWLEDGEMENTS

The authors are thankfull to Bardella SA Mechanical Industries for the micrographic analysis and to the Department of Structural Engineering (SET) of School of Engineering of São Carlos (EESC-USP) for the permission of using the computational cluster.

6. REFERENCES

Azevedo, C.R.F. and Hippert Jr, E., 2002. “Failure analysis of surgical implants in Brazil”. *Engineering Failure Analysis*, Vol. 9, p. 621.

Brooks, C.R., 1992. “Fatigue fracture of stainless steel wires in an electrostatic precipitator at a paper plant”. In: *Handbook of Case Studies in Failure Analysis, Vol. 1*. ASM International.

Bucholz, R.W. and Jones A., 1991. “Fractures of the shaft of the femur”. *J. Bone Joint Surg Am*, Vol. 73, p. 1561.

Castro, R. and Gueussier, A., 1960. “Embrittlement of austenitic steels”. *Revue Metalurgie*, Vol. 8.

Giordani, E.J., Guimarães, V.A., Pinto, T.B. and Ferreira, I., 2004. “Effect of precipitates on the corrosion-fatigue crack initiation of ISO 5832-9 stainless steel biomaterial”. *International Journal of Fatigue*, Vol. 26, p. 1129.

Hedlund R. and Lindgren U., 1986. “Epidemiology of diaphyseal femoral fracture”. *Acta Orthop Scand*, Vol. 57, p. 423.

Kanchanomai, C., Phiphobmongkol, V. and Muanjan, P., 2008. “Fatigue failure of an orthopaedic implant - a locking compression plate”. *Engineering Failure Analysis*, Vol. 15, p. 521.

Lee, Y.L., Pan, J., Hathaway, R. and Barkey, M., 2005. *Fatigue Testing and Analysis: Theory and Practice*. Elsevier, Amsterdam, 1st Edition.

Marcomini, J.B., Baptista, C.A.R.P., Pascon, J.P., Teixeira, R.L. and Reis, F.P., 2014. “Investigation of a fatigue failure in a stainless steel femoral plate”. *Journal of the Mechanical Behavior of Biomedical Materials*, Vol. 38, p. 52.

Pascon, J.P. and Coda, H.B., 2002. “Analysis of elastic functionally graded materials under large displacements via high-order tetrahedral elements”. *Finite Elements in Analysis and Design*, Vol. 50, p. 33.

Perren, S.M., 2002. “Evolution of the internal fixation of long bone fractures”. *The Journal of Bone & Joint Surgery*, Vol. 84B, p. 1093.

Roffey, P., 2012. “Case study: Failure of high nitrogen stainless steel femoral stem”. *Engineering Failure Analysis*, Vol. 20, p. 173.

Stevens, C.T. and Duis, H.J., 2008. “Plate osteosynthesis of simple forearm fractures: LCP versus DC plates”. *Acta Orthop Belg*, Vol. 74, p. 180.

Sudhakar, K.V., 2005. “Metallurgical investigation of a failure in 316L stainless steel orthopaedic implant”. *Engineering Failure Analysis*, Vol. 12, p. 249.

Suytino, B.A., Widodo, T.D., Mahardika, M., Dewo, P. and Salim, U.A., 2012. “Effect of cold working and sandblasting on the microhardness, tensile strength and corrosion resistance of AISI 316L stainless steel”. *International Journal of Minerals, Metallurgy and Materials*, Vol. 19, p. 1093.

Weiss, R.J., Montgomery, S.M., Al Dabbagh, Z. and Jansson, K.A., 2009. “National data of 6409 Swedish inpatients with femoral shaft fractures: stable incidence between 1998 and 2004”. *Injury*, Vol. 40, p. 304.

7. RESPONSIBILITY NOTICE

The authors are the only responsible for the printed material included in this paper.